RNA Biology

Publication details, including instructions for authors and subscription information:
http://www.tandfonline.com/loi/krnb20

A minimalist biosensor: Quantitation of cyclic Di-GMP using the conformational change of a riboswitch aptamer

Colleen A. Kellenberger[a], Jade Sales-Lee[a], Yuchen Pan[b], Madalee M. Gassaway[a], Amy E. Herr[b] & Ming C. Hammond[ac]

[a] Department of Chemistry, University of California, Berkeley, CA 94720 USA

[b] Graduate Program in Bioengineering, University of California San Francisco and University of California Berkeley, CA, 94720 USA

[c] Department of Molecular & Cell Biology, University of California, Berkeley, CA, 94720 USA

Accepted author version posted online: 26 Jun 2015.

To cite this article: Colleen A. Kellenberger, Jade Sales-Lee, Yuchen Pan, Madalee M. Gassaway, Amy E. Herr & Ming C. Hammond (2015): A minimalist biosensor: Quantitation of cyclic Di-GMP using the conformational change of a riboswitch aptamer, RNA Biology, DOI: 10.1080/15476286.2015.1062970

To link to this article: http://dx.doi.org/10.1080/15476286.2015.1062970

A Minimalist Biosensor: Quantitation of Cyclic Di-GMP Using the Conformational Change of a Riboswitch Aptamer

Colleen A. Kellenberger[1], Jade Sales-Lee[1], Yuchen Pan[2], Madalee M. Gassaway[1], Amy E. Herr[2], and Ming C. Hammond[1,3*]

1. Department of Chemistry, University of California, Berkeley, Berkeley, CA 94720 USA

2. Graduate Program in Bioengineering, University of California San Francisco and University of California Berkeley, CA, 94720 USA

3. Department of Molecular & Cell Biology, University of California, Berkeley, Berkeley, CA, 94720 USA

* corresponding author email: mingch@berkeley.edu

KEYWORDS:

Cyclic dinucleotides, cyclic AMP-GMP, bacterial signaling, microfluidic mobility shift assay, native EMSA, ligand binding

Abstract

Cyclic di-GMP (c-di-GMP) is a second messenger that is important in regulating bacterial physiology and behavior, including motility and virulence. Many questions

remain about the role and regulation of this signaling molecule, but current methods of detection are limited by either modest sensitivity or requirements for extensive sample purification. We have taken advantage of a natural, high affinity receptor of c-di-GMP, the Vc2 riboswitch aptamer, to develop a sensitive and rapid electrophoretic mobility shift assay (EMSA) for c-di-GMP quantitation that required minimal engineering of the RNA.

Introduction

Cyclic di-GMP (c-di-GMP) is a ubiquitous signaling molecule in bacteria that plays a role in virulence, motility and biofilm formation.[1] The molecule was first discovered by Benziman and coworkers in 1987 and has been the subject of extensive research, yet many questions remain about the components and mechanisms of signaling.[2–4] Recently, c-di-GMP and the other natural cyclic dinucleotides were shown to trigger an innate immune response in mammalian cells and thus, c-di-GMP is also a promising small molecule adjuvant.[5,6] In order to make further advances in studying c-di-GMP biology it is necessary that facile and accurate methods exist for measuring the concentration of this second messenger.

Key areas of c-di-GMP signaling that remain poorly understood include input signals that lead to c-di-GMP-dependent regulation, temporal resolution of c-di-GMP signaling, and an explanation for the high multiplicity of c-di-GMP metabolism enzymes in various bacteria.[7] Bioinformatic studies have shown that diguanylate cyclases and phosphodiesterases, which synthesize and degrade c-di-GMP, respectively, are highly abundant in bacteria; for example 29 synthase and/or degradase enzymes have been predicted in *E. coli* alone.[8] However, a full understanding of the regulation of these enzymes as well as how the global intracellular pool of c-di-GMP is affected by environmental signals is lacking. A general *in vitro* method for detecting c-di-GMP is advantageous because it can be applied for the study of virtually any organism, including genetically intractable organisms or mixed microbial populations, and ideally could detect changes in c-di-GMP concentration with high sensitivity.

Previously developed methods of detecting c-di-GMP in solution require extensive sample purification or have modest sensitivity. The commonly used HPLC-MS method has a lower limit of detection (LLOD) of 2 ng/mL or ~2 nM c-di-GMP but typically requires significant sample purification and is limited in high-throughput capability.[9] Other methods, including circular dichroism or small molecule-based detection methods, are more accessible but are based on the dimerization or G-quadruplex formation of c-di-GMP, and thus detect c-di-GMP at low micromolar concentrations.[10–12] Potential c-di-GMP binding proteins have been identified from whole cell lysates using the Differential Radial Capillary Action of Ligand Assay (DRaCALA), however this method uses radiolabeled ligand and is aimed at identification of protein-ligand interactions, not for quantification of endogenous ligand.[13]

Highly selective c-di-GMP fluorescent biosensors have been developed that take advantage of protein or RNA receptors that naturally bind c-di-GMP.[14–16] Protein-based biosensors use fusions of fluorescent proteins to PilZ domain-containing proteins, such as YcgR from *Salmonella enterica* and MrkH from *Klebsiella pneumoniae*, which give changes in Förster resonance energy transfer (FRET) upon binding c-di-GMP with reported dissociation constants (K_d) of 195 and 120 nM, respectively.[14,15] While these protein-based biosensors are useful for *in vivo* imaging of c-di-GMP, their use *in vitro* requires rigorous purification of the expressed protein from cellular extracts in order to remove any pre-bound c-di-GMP.

In contrast, one distinct advantage of riboswitch-based biosensors is the ability to synthesize RNAs by *in vitro* transcription, which eliminates the possibility of contaminating c-di-GMP from cellular extracts. A GEMM-I class riboswitch aptamer

upstream of a Tfox-like gene in *Vibrio cholerae* called Vc2 exhibits remarkably high affinity for c-di-GMP (K_d ~ 11 pM)[17,18] and has been fused to various output domains to create c-di-GMP sensors.[19,20] We[16] and others[21] have created fluorescent sensors by coupling the Vc2 aptamer to the Spinach aptamer,[22,23] an RNA mimic of GFP. Fusion of the Vc2 aptamer to Spinach either through its natural P1 stem (K_d ~ 8 ± 1 nM at 25 °C, 10 mM $MgCl_2$)[16] or an unnatural stem (K_d not reported, estimated high nanomolar)[21] results in a loss of affinity for c-di-GMP compared to the WT Vc2 aptamer alone. Alternatively, Breaker and coworkers have fused the Vc2 aptamer to a hammerhead ribozyme sequence through a random transducer stem and selected for allosteric c-di-GMP ribozyme sequences (affinities range from 70 to 500 nM).[20]

Together, these prior studies indicate the potential use of riboswitch aptamers for *in vitro* detection of c-di-GMP. However, a minimalist approach that uses the conformational change of the Vc2 aptamer alone had not yet been explored. We were interested to see whether it was possible to develop a ligand quantitation assay with such a “minimalist biosensor”, because it could accelerate the time between riboswitch discovery and application as a biosensor.

Here, we show that it is possible to perform *in vitro* quantitation of c-di-GMP using the Vc2 aptamer alone. A tetraloop mutant of the Vc2 aptamer (A33U Vc2) was found to display an increased mobility shift upon ligand binding that enabled detection down to ~100 pM of c-di-GMP, which is at least 20-fold more sensitive than previous methods. However, due to slow ligand equilibration rates and poor resolution of traditional slab gel EMSAs toward the separation of conformational states, this initial assay required nearly four days to complete. Through optimizing the binding reaction

parameters to considerably reduce equilibration time and converting to a microfluidic mobility shift assay (μMSA) to further reduce electrophoretic separation time,[24,25] the total assay time was improved to 30 min while low nanomolar sensitivity to c-di-GMP was maintained. Thus, in this technical paper, we illustrate a strategy for adapting riboswitch aptamers to the μMSA format as minimalist biosensors for detection of their target ligands.

Materials and Methods

Reagents and oligonucleotides

DNA oligonucleotides were purchased from Elim Biopharmaceuticals (Hayward, CA) and IDT (Coralville, IA). Cyclic di-GMP was purchased from Axxora, LLC (Farmingdale, NY). Commercially available reagents were used without further purification. Alexa Fluor 488-labeled trypsin inhibitor (TI) was purchased from Invitrogen (Waltham, MA).

In vitro transcription

DNA templates were made through PCR amplification using primers that added the T7 polymerase promoter sequence. The templates were transcribed using T7 RNA polymerase (NEB, Ipswich, MA) in 40 mM Tris-HCl, pH 8.0, 6 mM $MgCl_2$, 2 mM spermidine, and 10 mM DTT. RNA was purified by denaturing (7.5 M urea) 6% polyacrylamide gel electrophoresis (PAGE) and was extracted from gel pieces using Crush Soak buffer (10 mM Tris-HCl, pH 7.5, 200 mM NaCl and 1 mM EDTA, pH 8.0). RNAs were precipitated with ethanol and resuspended in TE buffer (10 mM Tris-HCl,

pH 8.0, 1 mM EDTA). Accurate RNA concentrations were determined via a thermal hydrolysis assay.[26]

Radiolabeling of RNA

In vitro transcribed RNA was dephosphorylated with alkaline phosphatase (Roche, Basel, Switzerland). The RNA was phenol/chloroform extracted and then ethanol precipitated overnight. RNAs were 5′-end labeled with γ-^{32}P ATP (Perkin Elmer, Waltham, MA) using T4 polynucleotide kinase (NEB) and were purified via PAGE as described previously.[27]

Native slab gel EMSAs

Reactions (10 µL) were prepared by mixing radiolabeled RNA (<100 pM or 1 µM) with c-di-GMP in buffer containing 89 mM Tris, pH 8.0, 89 mM boric acid, 1-10 mM $MgCl_2$, 100 mM KCl, and 1 mg/mL yeast extract. Reactions were incubated at room temperature for various times, then were mixed with 3 µL 50% glycerol before loading on a 10% native gel containing the same buffer. Gels were run for 14 h at 4 °C, then were dried, exposed on a phosphor cassette, and imaged using a Typhoon laser-scanning system (GE Healthcare).

Fluorescent RNA labeling

Alexa Fluor 488-labeled RNA was prepared as described previously.[28] Briefly, the 3′ end of the RNA was oxidized with sodium periodate and then AlexaFluor488 hydrazide (Life Technologies, Carlsbad, CA) was coupled to the RNA in sodium acetate buffer.

The RNA was precipitated in ethanol and then purified by PAGE as previously described.

Microfluidic device fabrication

As previously described,24 glass microfluidic chips were designed in-house and fabricated with standard wet etching process by Perkin Elmer (Hopkinton, MA). Prior to gel polymerization in-chip, each microchannel was washed with 1 M NaOH and silanized with a degased solution of 3-(trimethoxysilyl)-propyl methacrylate (Sigma Aldrich, St. Louis, MO), glacial acetic acid (Sigma Aldrich), and water (Mediatech, Menassas, VA) (2:3:5, v/v/v). The solution was introduced to the chip by capillary force. Photopatterning of polyacrylamide in the glass channels was conducted in-house according to our previously described process.24 A 3%T to 18%T discontinuous polyacrylamide gel (%T indicates the total concentration of acrylamide:bis, w/v; 3.3% was the weight percentage of bis-acrylamide in total monomer, w/w) was employed to enhance the separation resolution.

μMSA operation

The μMSA device is a glass microfluidic device comprised of two intersecting microchannels (80 μm deep × 20 μm wide), each terminating in fluid wells (Figure 4A). Fluid wells are notated as: reagent reservoir (RR), reagent waste (RW), buffer reservoir (BR), and buffer waste (BW). Pipette tips (1 cm long) were cut and placed into the wells to expand the reservoir volume. Run buffer (1X TBMK) contained 89 mM Tris, 89 mM boric acid, 3 mM $MgCl_2$, and 10 mM KCl. The binding reactions (10 μL) were prepared in 0.5 mL Eppendorf Lo-Bind tubes with the following final concentration of components: 1X

TBMK, 1 µM riboswitch RNA, 100 µg/mL yeast tRNA, 500 nM AlexaFluor 488 (AF488)-conjugated Trypsin Inhibitor (TI*) (Life Technologies, Carlsbad, CA), and indicated concentrations of c-di-GMP. Yeast tRNA is used to protect the riboswitch RNA from degradation by RNases. TI* was used as an internal standard. The mixture was heated at 70 °C for 3 min and cooled for 10 min at room temperature to renature the RNAs before the addition of c-di-GMP and TI*. The riboswitch binding reaction was incubated off-chip in a tube, and a 4 µL sample was pipetted into the RR. All other wells were filled with 4 µL of 1X TBMK buffer. Platinum electrodes were inserted into each well and were connected to a custom built, 8-channel high voltage power supply with current/voltage feedback control. The µMSA was performed in constant current mode. First, samples were loaded into the microchannel by applying -12 µA to the RR, and electrophoresed into the RR-to-RW microchannel by applying -2 µA to BR and BW as pinching voltage and grounding RW for 1 min. After the loading process was stabilized, the voltage plan was switched to sample injection/separation, by applying -32 µA to BR, 10 µA to RR and RW as pulling voltage and grounding BW. The result is injection of a plug of sample into the separation channel at the t-junction and the sample is electrophoresed into the BR-to-BW microchannel, which houses a 3-18 %T discontinuous sample stacking and separation gel.

µMSA imaging and data analysis

Full-field images of peak migration and fluorescence were collected via an Olympus IX-70 inverted epi-fluorescence microscope equipped with a Peltier cooled charge-coupled device (CCD) camera (CoolSNAP HQ2, Roper Scientific, Trenton, NJ) and a 10X

objective. An X-Cite1 exacte mercury lamp (Lumen Dynamics, Mississauga, Canada) provided the illumination source, which was then filtered by an XF100-3 filter (Omega Optical, Brattleboro, VT). In equilibrium time studies, the camera exposure time was 100 ms. For concentration calibration, electrophoresis was monitored in real time and halted when the unshifted RNA band migrated to the 1 mm marker, followed by collection of a 500 ms exposure image.

Images were analyzed using ImageJ software (NIH, Bethesda, MD). Fluorescence intensity was collected along the axis of the separation channel and averaged in the transverse direction. Post-processing was performed with OriginPro 8.0 (OriginLab, Northampton, MA). A built-in non-linear Gaussian peak-fitting algorithm was employed to calculate peak position and area-under-the-curve (AUC) from the axial fluorescence signal. To quantify the amount of bound riboswitch, we introduced TI as an internal standard molecule. Instead taking the absolute value of AUC of the bound riboswitch, we normalized it to that of TI therefore minimizing the run-to-run variation. Signal-to-noise ratio (SNR) was calculated by dividing the maximum intensity value of the Gaussian fit by the root mean square (r.m.s) noise of neighboring regions of signal. Peaks were considered detectable when SNR > 3, as per convention.

Cell extraction of *E. coli*

E. coli strains from the Keio collection[29] were obtained from the *E. coli* Genetic Stock Center (Yale University). The wild-type *E. coli* K-12 strain was BW25113 [*F-, Δ(araD-araB)567*, *ΔlacZ4787(::rrnB-3), λ–, rph-1, Δ(rhaD-rhaB)568, hsdR514*]. Mutant strains

were isogenic derivatives of BW25113 and included JW1278-1 *(*Δ*gmr-722::kan*), JW2052-1 (Δ*yegE-765::kan*), JW3493-2 (Δ*yhjH-780::kan*), JW5291-1 (Δ*yeaJ-783::kan*). Fresh cultures of 15 mL of LB (BW25113) or LB/kanamycin (mutant strains, 50 µg/mL kanamycin) were inoculated 1:40 with overnight cultures grown at 37 °C. Cultures were grown in a 37 °C incubator with shaking for approx. 7 h, then the OD_{600} was measured and cell pellets were collected by centrifugation at 6,500 rpm for 10 min at 4 °C. An organic-aqueous extraction of cell pellets was performed as described previously.[9] Briefly, the pellets were resuspended using 600 µL acetonitrile/methanol/water (40/40/20, v/v/v) on ice for 20 min with occasional vortexing. The suspension was further extracted at ambient temperature for 20 min, then cell debris was pelleted with centrifugation at 13,200 rpm for 20 min at 4 °C. The supernatant was carefully removed and stored on ice and the pellet was extracted twice more with 300 µL extraction buffer. The combined supernatants were evaporated to dryness by rotary evaporation and the dried material was resuspended in 200 µL deionized H_2O. For analysis by µMSA, 5 µL of concentrated extract was added to bring the final volume of the riboswitch binding reaction to 10 µL (final concentrations of other components are 1 µM AF488-labelled RNA, 100 µg/ml tRNA, 1X TBMK buffer, and 500 nM TI*). The reported c-di-GMP concentration values are for the concentrated cell extract, take into account the 2X dilution factor, and are normalized to OD_{600}.

Results

A tetraloop mutant of the Vc2 aptamer demonstrates an increased electrophoretic mobility shift

Conventional EMSAs are based upon separation of different molecular weight species. For example, formation of the riboswitch aptamer-ligand complex using Vc2 RNA and radiolabeled c-di-GMP has been observed by native EMSA, which relies on the large electrophoretic mobility difference between free and complexed c-di-GMP.[18,19,30] Smith *et al.* employed a competition binding experiment to analyze binding of unlabeled ligands.[18] However, these types of assays typically have poorer limits of detection than direct binding assays, since low levels of c-di-GMP inefficiently compete with the labeled ligand.

Although less common, native EMSAs also can be used to separate different radiolabeled RNA conformations induced by ligand binding (Figure 1A). This method requires labeled RNA but enables unlabeled ligands to be interrogated by direct binding experiments, which is important for quantifying c-di-GMP from natural sources, evaluating potential ligand candidates,[31] or identifying small molecule inhibitors of riboswitch activity.[32] Previous studies using small angle x-ray scattering (SAXS) and single molecule FRET (smFRET) experiments have shown that the Vc2 aptamer undergoes a significant structural compaction upon binding c-di-GMP.[19,30] Specifically, in an unbound state, the majority of RNAs are in an elongated conformation with distal P2 and P3 stems, but when bound to c-di-GMP, these two stems form tertiary interactions that result in a more globular architecture. This structural compaction has been used by Kulshina *et al.* to determine the specificity of the RNA for c-di-GMP over other nucleotide analogs through native EMSA.[30]

In contrast to a binary plus/minus binding assay, we sought to develop an assay that would allow for highly sensitive quantitation of c-di-GMP. Determination of c-di-

GMP concentrations through EMSA requires resolution of the bound and unbound bands for accurate quantitation. Thus, optimization efforts sought to increase the observed mobility shift upon ligand binding. Specifically, we analyzed two strategies for affecting RNA structure: the effects of altering Mg^{2+} concentrations and of weakening a tertiary interaction. Magnesium ions mediate binding of c-di-GMP to the Vc2 aptamer and have been shown to affect mobility shifts of another riboswitch aptamer.[19,33] In addition, one tertiary interaction that stabilizes the globular structure of the bound Vc2 riboswitch is a tetraloop/tetraloop receptor interaction between the P2 and P3 stems.[18,30] An A33U mutation to the tetraloop in the P2 stem loop of Vc2 impairs a base-stacking interaction with the tetraloop receptor in the P3 stem, therefore weakening the ability of this tertiary interaction to form (Figure 1B).[19,34]

Radiolabeled WT and A33U Vc2 aptamer RNAs were incubated in buffers with varied $MgCl_2$ concentrations either with or without an excess of c-di-GMP, then were separated on native slab polyacrylamide gels containing the corresponding concentration of $MgCl_2$ (Figures 1C and S1). Under all three Mg^{2+} conditions tested, the WT Vc2 aptamer shows a smaller relative mobility shift upon binding c-di-GMP than the A33U Vc2 aptamer. Interestingly, the main difference in relative mobility shift comes from decreased mobility of the A33U aptamer in the unbound state, an effect that is enhanced with lower magnesium concentrations (Table 1). In contrast, the mobility of the c-di-GMP bound WT and A33U Vc2 RNAs is nearly equal within each gel, suggesting that the A33U mutation reduces compactness of the unbound aptamer, but that addition of c-di-GMP restores the structure to match the mobility of WT Vc2.

In addition, Mg^{2+} concentration impacts both the absolute and relative electrophoretic mobility of the aptamers (Figures 1C and S1). First, decreasing the $MgCl_2$ concentration led to increased electrophoretic velocities for all RNAs. Intuitively, this effect is due to reduced shielding by magnesium ions of the negatively charged RNA backbone. Theoretically, decreasing ionic strength increases the Debye length of the electric double layer around the molecule, as reflected in an altered zeta potential (φ_0). The magnitude of the electrophoretic mobility is proportional with φ_0, given by $\mu = \varepsilon E \varphi_0 / \eta$, in which ε is the permittivity of the electrolyte solution, *E* is the electric field strength and η is the dynamic viscosity. Increased ionic strength can also lead to Joule heating, which may alter the dynamic viscosity. Second, decreasing the Mg^{2+} concentration also yielded larger separations between the bound and unbound RNA conformations for both WT and A33U Vc2 RNAs (Table 1), although the effect is more pronounced for the A33U mutant. Thus, lowering the $MgCl_2$ concentration affects both the absolute electrophoretic velocities and the relative mobility shift of each species, thus enhancing the separation resolution between bound and unbound species.

The electrophoretic mobility shift assay allows for high picomolar detection of c-di-GMP

A slow off-rate (1.1 x 10^{-5} min^{-1}) has been reported for c-di-GMP dissociation from the WT riboswitch aptamer under buffer conditions with 10 mM $MgCl_2$.[18] Thus, not only does the WT aptamer have a reduced mobility shift compared to A33U Vc2, but the time for the binding reaction to reach equilibrium (ca. months) renders WT Vc2 impractical for c-di-GMP quantitation. In contrast, the binding reaction between A33U

Vc2 (<100 pM) and non-saturating concentrations of c-di-GMP reaches equilibrium after ~75 h of incubation (Figure 2A). Similar equilibration times were observed for reactions whether incubated in buffer with 10 mM $MgCl_2$ and 10 mM KCl or 3 mM $MgCl_2$ and 3 mM KCl, indicating that in this range of ionic concentrations there was little effect on kinetics (Figures 2A and S2). Thus, we used a 75 h incubation time for experiments to determine the sensitivity of c-di-GMP detection.

While lowering Mg^{2+} levels leads to a larger electrophoretic mobility shift between bound and unbound species, reduced Mg^{2+} levels also result in poorer binding affinity for c-di-GMP (Figures 2B-C). At 1 mM $MgCl_2$ the affinity of A33U Vc2 for c-di-GMP is in the nanomolar regime (K_d value of 1.6 ± 0.1 nM), whereas sub-nanomolar affinity is achieved at 3 and 10 mM $MgCl_2$ (K_d values of 520 ± 30 pM and 210 ± 10 pM, respectively). The LLOD for c-di-GMP is ~100 pM with 10 mM $MgCl_2$ (SNR > 3) (Figure 2B), which is an order of magnitude lower than the most sensitive existing methods.[9,35] However, as a compromise between resolution and binding affinity, further optimization of the assay was performed with 3 mM $MgCl_2$. Under these conditions, the dynamic range of detection between 10-90% of the fraction bound is 55-4400 pM c-di-GMP, providing a method for quantifying low levels of c-di-GMP with high accuracy. Furthermore, preliminary data shows that mutants of the Vc2 aptamer enable adaptation of this assay for detection of the recently discovered second messenger 3′-5′, 3′-5′ c-AMP-GMP (Figure S3), which has been implicated in the regulation of *Vibrio cholerae* virulence[36] and *Geobacter* extracellular electron transport.[37,38]

Optimization of the slab gel EMSA and conversion to μMSA allows for more rapid and sensitive detection of c-di-GMP

We considered that the long equilibrium incubation time (~75 h) is not only a function of the rate constants but is also dependent on the concentrations of RNA and ligand in the binding reaction. In order to reduce the time to reach equilibrium, the addition of excess unlabeled riboswitch aptamer in the radiolabeled binding reactions was analyzed. For example, in a binding reaction containing a total RNA concentration of 1.1 μM A33U Vc2 with 100 nM c-di-GMP, equilibrium was reached within 30 min (Figure 3A), which is a 150-fold decrease in incubation time compared to previous experiments using <100 pM of A33U Vc2 with 1 nM c-di-GMP, albeit under slightly different $MgCl_2$ concentrations (Figure 2A).

With the addition of excess RNA, the amount of the Vc2 aptamer greatly exceeds the dissociation constant, so the signal from bound RNA becomes directly proportional to the amount of c-di-GMP present in the sample. Importantly, the measurement of c-di-GMP concentrations no longer depends on the fraction of RNA bound, but solely on the amount of RNA that is shifted to the bound state (as excess RNA remains largely unbound at low levels of c-di-GMP). This method was used to generate a standard curve for c-di-GMP detection (Figure 3B). The LLOD for c-di-GMP under these conditions is ~5 nM, which matches that of current HPLC-MS methods,[9,35] and has a linear response to increased c-di-GMP levels up to 400 nM as shown here.

While the reaction equilibration time was decreased, performing the separation on the slab gel still required 12-14 h of gel electrophoresis at 4 °C. To reduce electrophoresis time, we converted to the microfluidic mobility shift assay (μMSA) format

(Figure 4A). This technique provides rapid, resource-sparing, and reproducible results using fluorescently-labeled RNA without the precautions required for radiolabeled materials.[24] As shown, separation of bound and unbound A33U Vc2 aptamer labeled at the 3′ end with Alexa Fluor 488 was achieved in 30 seconds at room temperature, a ~1,440-fold decrease in the separation time (Figure 4B). Meanwhile, the same equilibration time of 30 min was found when monitoring the binding reaction by μMSA (Figure 4C).

A standard curve for c-di-GMP detection was generated via μMSA using 1 μM Alexa Fluor 488-labeled RNA with c-di-GMP concentrations ranging from 1-1000 nM (Figure 4D). The amount of bound RNA was observed to increase linearly with the concentration of c-di-GMP, and the LLOD is 10 nM c-di-GMP (S/N ratio ~6.7) (Figure S4). Thus, on the microfluidics platform, we are able to achieve comparable sensitivity and similar linearity of response relative to the slab gel format. The aforementioned advantages of the μMSA format along with the ~216,000-fold reduction in experiment time makes this assay advantageous for highly sensitive and rapid detection of unlabeled c-di-GMP.

Previously, deletion mutants of two phosphodiesterases, Gmr (also called YciR) and YhjH, and two diguanylate cyclases, YegE and YeaJ, in different *E. coli* strains have been shown to affect biofilm formation and/or motility phenotype.[39–41] Specifically, we expected that knocking out the phosphodiesterases would increase c-di-GMP concentrations, leading to increased biofilm staining and decreased motility in soft agar assays. In contrast, we expected that knocking out the diguanylate cyclases would decrease c-di-GMP concentrations, leading to the opposite phenotypes. The phenotypic

observations for these mutants and, in the case of Δ*gmr*, allosteric ribozyme reporter assays,[42] have been consistent with the predicted changes in c-di-GMP concentrations. However, to our knowledge, the c-di-GMP concentrations for these mutant strains had not been directly measured.

To analyze endogenous c-di-GMP levels, we performed an organic-aqueous extraction of cell pellets from Keio collection strains grown to stationary phase (OD_{600} ~3) in 15 mL of LB liquid culture without or with kanamycin (for mutants), following previously described procedures.[9,37] The strains analyzed were BW25113, the wild-type *E. coli* K-12 strain, and isogenic derivatives of BW25113 with the following single gene deletions: Δ*gmr*, Δ*yhjH*, Δ*yegE*, and Δ*yeaJ*. We then attempted to quantify c-di-GMP levels directly from these crude cell extracts via μMSA with the fluorescently labeled A33U Vc2 aptamer. Triplicate runs on the μMSA platform gave consistent values for each sample, but we unfortunately observed high variability between two independent biological replicates from experiments performed on different days (Figure S5). Also in retrospect, the Keio strains were not the same strains used in the phenotype assays, and the growth conditions were different as well. These differences may change the expected c-di-GMP concentrations, as *E. coli* harbor multiple diguanylate cyclases and phosphodiesterases (up to 29) whose expression levels are influenced by growth conditions.[1]

Discussion

Here we present a minimalist approach toward biosensor development that focused on *in vitro* detection of c-di-GMP using the Vc2 riboswitch aptamer alone. Numerous riboswitch aptamers exhibit low nanomolar affinities toward their cognate

ligands[17,43] and undergo a conformational change upon ligand binding, so this study details the assay development steps necessary and serves as a proof-of-principle for c-di-GMP detection. Recently, we also have used a SAM-I riboswitch aptamer to verify *S*-adenosylmethionine levels in yeast cell extracts through standard EMSA.[44] Together, these studies show that the conformational shift of riboswitch aptamers, which has previously been used to study RNA structure and folding,[45] can be used to quantify their small molecule ligands.

One key characteristic of the Vc2 aptamer is its unusually slow ligand off-rate,[18] which is over four orders of magnitude slower than the reported off-rates for the adenine and FMN riboswitches.[46,47] Slow ligand dissociation contributes to the high sensitivity of the aptamer for c-di-GMP and the observation of distinct bands for ligand-bound and unbound states, as ligand dissociation is slower than the rate of separation by electrophoresis. We found that the A33U Vc2 tetraloop was useful to enhance electrophoretic separation of the two species. Previous affinity studies of the A33U Vc2 aptamer reported a 200-fold decrease in c-di-GMP affinity,[34] attributed to an increase in the off-rate. This A33U Vc2 mutation destabilizes an important tertiary interaction whereas other disruptive mutations mainly facilitate unbinding of the ligand.[34] Single molecule studies have shown that this tetraloop mutation results in an increase in the amount of statically undocked RNAs, in which the P2 and P3 stems are distal, agreeing with this RNA being in a less compact formation when not bound to c-di-GMP.[19]

We found that an intermediate (3 mM) magnesium concentration maintains strong c-di-GMP binding affinity and still provides sufficient destabilization of the unbound aptamer structure to produce an improved mobility shift. Previous studies of

the Vc2 aptamer have linked low magnesium concentration to reduced ligand binding affinity.[16,19,30] The crystal structure of the c-di-GMP bound riboswitch aptamer revealed that magnesium coordinates with c-di-GMP in the ligand binding pocket and SAXS studies showed low magnesium concentration correlates with increased global size.[30,34]

Finally, in order to reduce the assay time, we switched from a "fraction bound" type of binding assay that uses RNAs at concentrations below the K_d value to a "standard curve" type of binding assay that uses RNAs at stoichiometric concentrations. This modification in assay protocol, in combination with the adoption of the μMSA format, provides an assay that can be accomplished in practical time-scales and with low amounts of fluorescently labeled RNAs. The fluorophore labeling procedure can be performed on *in vitro* transcribed RNAs of any length, and the sequence at the 3' end can be extended as necessary to avoid perturbation of ligand binding to the aptamer (Figure 1B). We demonstrate that μMSA matches the limit of detection of the most sensitive existing techniques for c-di-GMP quantification.

In the future, we expect that further method optimization and normalization controls will be required to quantify c-di-GMP accurately from crude bacterial extracts, as opposed to extensively purified standards. However, our preliminary results do suggest that the assay will have the sensitivity to detect c-di-GMP from small batches of cell extracts. The high variability in independent replicates point out that a main challenge in fact may be accounting for differences in biological samples and in extraction efficiency. A potential solution would be to measure a larger number of replicates so that any statistically significant differences can be reliably assessed. Promisingly, the format offers the possibility for high-throughput screening, as a free-

standing polyacrylamide gel device recently has been described that enables 96-well multiplexing of μMSA for sample analysis.[25]

References

1. Hengge R. Principles of c-di-GMP signalling in bacteria. Nat Rev Microbiol 2009; 7:263–73.

2. Ross P, Weinhouse H, Aloni Y, Michaeli D, Weinberger-Ohana P, Mayer R, Braun S, do Vroom E, van der Marel GA, van Boom JH, et al. Regulation of cellulose synthesis in Acetobacter xylinum by cyclic diguanylic acid. Nature 1987; 325:279–81.

3. Düvel J, Bertinetti D, Möller S, Schwede F, Morr M, Wissing J, Radamm L, Zimmermann B, Genieser H-G, Jänsch L, et al. A chemical proteomics approach to identify c-di-GMP binding proteins in Pseudomonas aeruginosa. J Microbiol Methods 2012; 88:229–36.

4. Massie JP, Reynolds EL, Koestler BJ, Cong J-P, Agostoni M, Waters CM. Quantification of high-specificity cyclic diguanylate signaling. Proc Natl Acad Sci U S A 2012; 109:12746–51.

5. Burdette DL, Monroe KM, Sotelo-Troha K, Iwig JS, Eckert B, Hyodo M, Hayakawa Y, Vance RE. STING is a direct innate immune sensor of cyclic di-GMP. Nature 2011; 478:515–8.

6. Svindland SC, Pedersen GK, Pathirana RD, Bredholt G, Nøstbakken JK, Jul-Larsen A, Guzmán C a, Montomoli E, Lapini G, Piccirella S, et al. A study of Chitosan and c-di-GMP as mucosal adjuvants for intranasal influenza H5N1 vaccine. Influenza Other Respi Viruses 2012; :1–13.

7. Römling U, Galperin MY, Gomelsky M. Cyclic di-GMP : the First 25 Years of a Universal Bacterial Second Messenger. Microbiol Mol Biol Rev 2013; 77:1–52.

8. Seshasayee ASN, Fraser GM, Luscombe NM. Comparative genomics of cyclic-di-GMP signalling in bacteria: post-translational regulation and catalytic activity. Nucleic Acids Res 2010; 38:5970–81.

9. Spangler C, Böhm A, Jenal U, Seifert R, Kaever V. A liquid chromatography-coupled tandem mass spectrometry method for quantitation of cyclic di-guanosine monophosphate. J Microbiol Methods 2010; 81:226–31.

10. Stelitano V, Brandt A, Fernicola S, Franceschini S, Giardina G, Pica A, Rinaldo S, Sica F, Cutruzzolà F. Probing the activity of diguanylate cyclases and c-di-GMP phosphodiesterases in real-time by CD spectroscopy. Nucleic Acids Res 2013; 41:e79.

11. Nakayama S, Kelsey I, Wang J, Roelofs K, Stefane B, Luo Y, Lee VT, Sintim HO. Thiazole orange-induced c-di-GMP quadruplex formation facilitates a simple fluorescent detection of this ubiquitous biofilm regulating molecule. J Am Chem Soc 2011; 133:4856–64.

12. Nakayama S, Roelofs K, Lee VT, Sintim HO. A C-di-GMP–proflavine–hemin supramolecular complex has peroxidase activity-implication for a simple colorimetric detection. Mol Biosyst 2012; 8:726–9.

13. Roelofs KG, Wang J, Sintim HO, Lee VT. Differential radial capillary action of ligand assay for high-throughput detection of protein-metabolite interactions. Proc Natl Acad Sci U S A 2011; 108:15528–33.

14. Christen M, Kulasekara HD, Christen B, Kulasekara BR, Hoffman LR, Miller SI. Asymmetrical distribution of the second messenger c-di-GMP upon bacterial cell division. Science 2010; 328:1295–7.

15. Ho CL, Chong KSJ, Oppong JA, Chuah MLC, Tan SM, Liang Z-X. Visualizing the perturbation of cellular cyclic di-GMP levels in bacterial cells. J Am Chem Soc 2013; 135:566–9.

16. Kellenberger CA, Wilson SC, Sales-Lee J, Hammond MC. RNA-based fluorescent biosensors for live cell imaging of second messengers cyclic di-GMP and cyclic AMP-GMP. J Am Chem Soc 2013; 135:4906–9.

17. Sudarsan N, Lee ER, Weinberg Z, Moy RH, Kim JN, Link KH, Breaker RR. Riboswitches in eubacteria sense the second messenger cyclic di-GMP. Science 2008; 321:411–3.

18. Smith KD, Lipchock S V, Ames TD, Wang J, Breaker RR, Strobel SA. Structural basis of ligand binding by a c-di-GMP riboswitch. Nat Struct Mol Biol 2009; 16:1218–23.

19. Wood S, Ferré-D'Amaré AR, Rueda D. Allosteric tertiary interactions preorganize the c-di-GMP riboswitch and accelerate ligand binding. ACS Chem Biol 2012; 7:920–7.

20. Gu H, Furukawa K, Breaker RR. Engineered Allosteric Ribozymes That Sense the Bacterial Second Messenger Cyclic Diguanosyl 5′-Monophosphate. Anal Chem 2012; 84:4935–41.

21. Nakayama S, Luo Y, Zhou J, Dayie TK, Sintim HO. Nanomolar fluorescent detection of c-di-GMP using a modular aptamer strategy. Chem Commun (Camb) 2012; 48:9059–61.

22. Paige JS, Wu KY, Jaffrey SR. RNA Mimics of Green Fluorescent Protein. Science 2011; 333:642–6.

23. Paige JS, Nguyen-Duc T, Song W, Jaffrey SR. Fluorescence Imaging of Cellular Metabolites with RNA. Science 2012; 335:1194.

24. Karns K, Vogan JM, Qin Q, Hickey SF, Wilson SC, Hammond MC, Herr AE. Microfluidic Screening of Electrophoretic Mobility Shifts Elucidates Riboswitch Binding Function. J Am Chem Soc 2013; 135:3136–43.

25. Pan Y, Duncombe TA, Kellenberger CA, Hammond MC, Herr AE. High-throughput electrophoretic mobility shift assays for quantitative analysis of molecular binding reactions. Anal Chem 2014; 86:10357–64.

26. Wilson SC, Cohen DT, Wang XC, Hammond MC. A neutral pH thermal hydrolysis method for quantification of structured RNAs. RNA 2014; 20:1153–60.

27. Regulski EE, Breaker RR. In-line probing analysis of riboswitches. Methods Mol Biol 2008; 419:53–67.

28. Willkom D, Hartmann RK, Bindereif A, Schön A, Westhof E. Handbook of RNA Biochemistry. Wiley 2005; 1:86.

29. Baba T, Ara T, Hasegawa M, Takai Y, Okumura Y, Baba M, Datsenko K A, Tomita M, Wanner BL, Mori H. Construction of Escherichia coli K-12 in-frame, single-gene knockout mutants: the Keio collection. Mol Syst Biol 2006; 2:2006.0008.

30. Kulshina N, Baird NJ, Ferré-D'Amaré AR. Recognition of the bacterial second messenger cyclic diguanylate by its cognate riboswitch. Nat Struct Mol Biol 2009; 16:1212–7.

31. Shanahan CA, Gaffney BL, Jones RA, Strobel SA. Differential Analogue Binding by Two Classes of c-di-GMP Riboswitches. J Am Chem Soc 2011; 133:15578–92.

32. Blount KF, Breaker RR. Riboswitches as antibacterial drug targets. Nat Biotechnol 2006; 24:1558–64.

33. Heppell B, Lafontaine DA. Folding of the SAM Aptamer is Determined by the Formation of a K-turn-dependent Pseudoknot. Biochemistry 2008; 47:1490–9.

34. Smith KD, Lipchock S V, Livingston AL, Shanahan CA, Strobel SA. Structural and biochemical determinants of ligand binding by the c-di-GMP riboswitch . Biochemistry 2010; 49:7351–9.

35. Simm R, Morr M, Remminghorst U, Andersson M, Romling U. Quantitative determination of cyclic diguanosine monophosphate concentrations in nucleotide extracts of bacteria by matrix-assisted laser desorption/ionization–time-of-flight mass spectrometry. Anal Biochem 2009; 386:53–8.

36. Davies BW, Bogard RW, Young TS, Mekalanos JJ. Coordinated Regulation of Accessory Genetic Elements Produces Cyclic Di-Nucleotides for V. cholerae Virulence. Cell 2012; 149:358–70.

37. Kellenberger* CA, Wilson* SC, Hickey SF, Gonzalez TL, Su Y, Hallberg ZF, Brewer TF, Iavarone AT, Carlson HK, Hsieh Y-F, et al. GEMM-I Riboswitches from Geobacter Sense the Bacterial Second Messenger cyclic AMP-GMP. Proc Natl Acad Sci U S A 2015; 112:5383–8.

38. Nelson JW, Sudarsan N, Phillips GE, Stav S, Lünse CE, McCown PJ, Breaker RR. Control of Exoelectrogenesis in Geobacter spp. by c-AMP-GMP. Proc Natl Acad Sci U S A 2015; 112:5389–94.

39. Weber H, Pesavento C, Possling A, Tischendorf G, Hengge R. Cyclic-di-GMP-mediated signalling within the σS network of Escherichia coli. Mol Microbiol 2006; 62:1014–34.

40. Pesavento C, Becker G, Sommerfeldt N, Possling A, Tschowri N, Mehlis A, Hengge R. Inverse regulatory coordination of motility and curli-mediated adhesion in Escherichia coli. Genes Dev 2008; 22:2434–46.

41. Sommerfeldt N, Possling A, Becker G, Pesavento C, Tschowri N, Hengge R. Gene expression patterns and differential input into curli fimbriae regulation of all GGDEF/EAL domain proteins in Escherichia coli. Microbiology 2009; 155:1318–31.

42. Chen AGY, Sudarsan N, Breaker RR. Mechanism for gene control by a natural allosteric group I ribozyme. RNA 2011; 17:1967–72.

43. Nelson JW, Sudarsan N, Furukawa K, Weinberg Z, Wang JX, Breaker RR. Riboswitches in eubacteria sense the second messenger c-di-AMP. Nat Chem Biol 2013; 9:834–9.

44. Sadhu MJ, Guan Q, Sales-Lee J, Iavarone AT, Hammond MC, Cande WZ, Rine J. Nutritional control of epigenetic processes in yeast and human cells. Genetics 2013; 195:831–44.

45. Eschbach SH, Lafontaine DA. RNA Conformational Changes Analyzed by Comparative Gel Electrophoresis. Methods Mol Biol 2014; 1086:255–64.

46. Wickiser JK, Cheah MT, Breaker RR, Crothers DM. The kinetics of ligand binding by an adenine-sensing riboswitch. Biochemistry 2005; 44:13404–14.

47. Wickiser JK, Winkler WC, Breaker RR, Crothers DM. The Speed of RNA Transcription and Metabolite Binding Kinetics Operate an FMN Riboswitch. Mol Cell 2005; 18:49–60.

Table 1. Distance traveled by WT and A33U Vc2 RNAs under various $MgCl_2$ concentrations. Data were obtained by measuring the distance of the bands shown in Figure 1C from the well of the gel using ImageJ software.

	10 mM $MgCl_2$	**3 mM $MgCl_2$**	**1 mM $MgCl_2$**
WT Vc2 – c-di-GMP	9.82 cm	11.14 cm	12.75 cm
WT Vc2 + c-di-GMP	9.93 cm	11.35 cm	13.11 cm
A33U Vc2 – c-di-GMP	9.37 cm	10.54 cm	11.77 cm
A33U Vc2 + c-di-GMP	9.98 cm	11.28 cm	12.95 cm

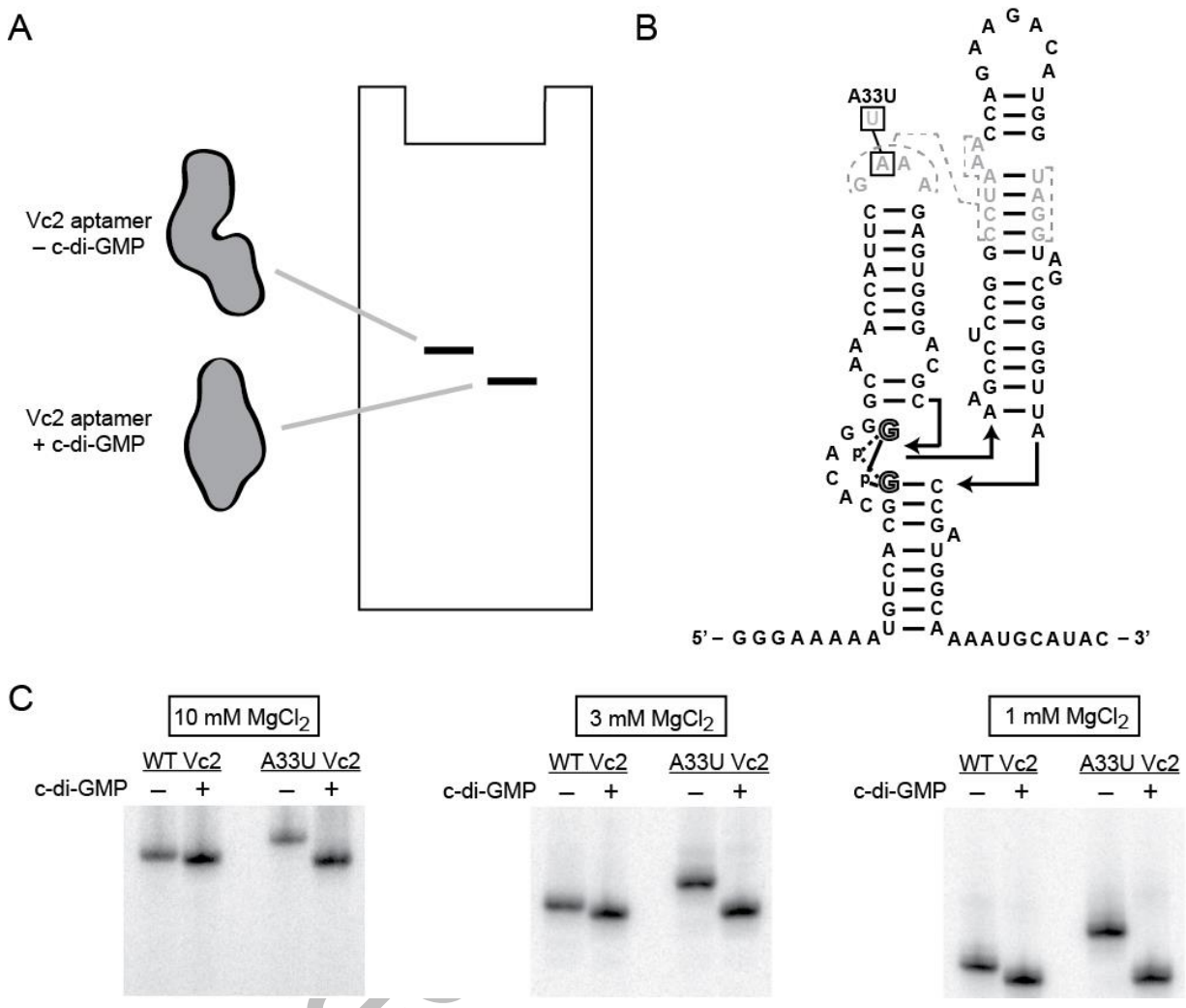

Figure 1. An A33U mutation leads to a larger electrophoretic mobility shift of the Vc2 aptamer with dependence on Mg^{2+} concentration. (A) Model of the conformational change resolved by an electrophoretic mobility shift assay. The global RNA conformations are outlines of structures previously solved by SAXS. (B) Sequence and secondary structure of the Vc2 aptamer. The A33U mutation is boxed and c-di-GMP is in large letters. The tetraloop-tetraloop receptor interaction is shown in dashed lines and nucleotides involved in this tertiary interaction are in gray. (**C**) EMSA of WT and A33U Vc2 RNAs with or without c-di-GMP run in 10 mM, 3 mM, or 1 mM $MgCl_2$.

Approximately 1 nM ^{32}P A33U Vc2 was incubated with 10 μM c-di-GMP for 4 h before loading on 10% polyacrylamide gels run for the same amount of time (14 h) at 4 °C. Images encompass the area 8.5 – 13.5 cm from the top of the gels.

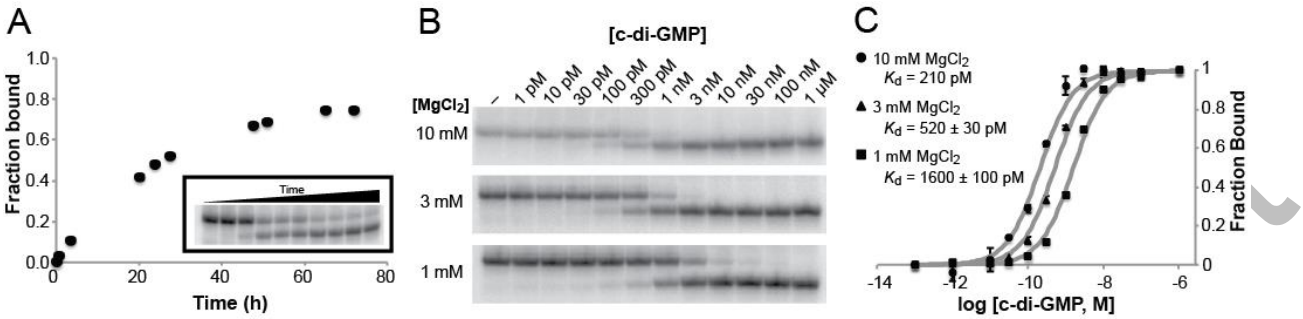

Figure 2. The A33U Vc2 aptamer detects high picomolar levels of c-di-GMP. (A) Analysis of A33U Vc2 equilibration time with c-di-GMP. Less than 100 pM ^{32}P A33U Vc2 RNA was incubated with 1 nM c-di-GMP for various times before loading on a 10% polyacrylamide gel run for 14 h at 4 °C in buffer containing 10 mM $MgCl_2$ and 10 mM KCl. (B) EMSAs of A33U Vc2 with c-di-GMP under different $MgCl_2$ concentrations. Less than 100 pM ^{32}P A33U Vc2 was incubated with various concentrations of c-di-GMP for 75 h before separating on a 10% polyacrylamide gel run for 14 h at 4 °C. (C) Analysis of A33U Vc2 affinity for c-di-GMP under various $MgCl_2$ concentrations. Data from two or three independent replicates and the best-fit curves are shown.

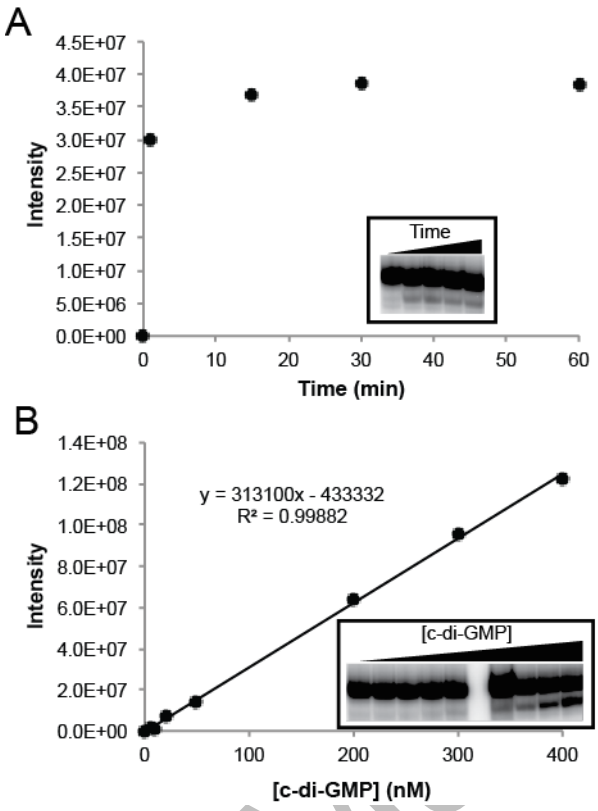

Figure 3. Addition of excess RNA decreases equilibration time while maintaining low nanomolar sensitivity. (A) Analysis of equilibration time required for an excess of A33U Vc2 to bind c-di-GMP. Approximately 100 pM ^{32}P A33U Vc2 was mixed with 1 μM unlabeled RNA and 100 nM c-di-GMP then was incubated for various times before loading on a 10% native polyacrylamide gel run for 14 h at 4 °C. The gel image insert shows the data points analyzed. (B) Standard curve of c-di-GMP binding A33U Vc2. Various concentrations of c-di-GMP were incubated with approximately 100 pM ^{32}P A33U Vc2 and 1 μM unlabeled RNA and 100 nM c-di-GMP for 30 min before loading on a 10% native polyacrylamide gel run for 14 h at 4 °C. The image of the gel analyzes is shown in the insert; the 6th and 7th lanes were excluded from analysis as they were a result of a gel loading error.

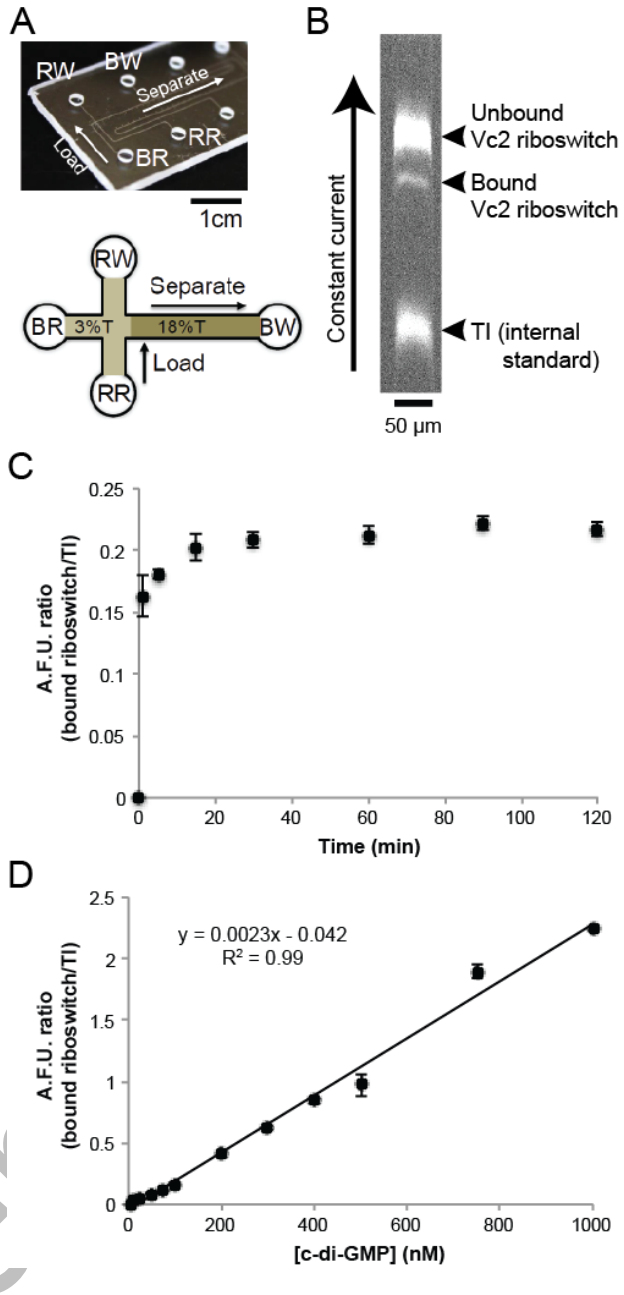

Figure 4. Conversion to a µMSA allows for rapid separation of conformational states and low nanomolar c-di-GMP detection. (A) Upper is photograph of the µMSA glass chip. Microchannel network is comprised of two intersecting microchannels, each terminating in a fluid reservoir. Reservoirs are: buffer reservoir, BR; riboswitch reservoir, RR; riboswitch waste, RW and buffer waste, BW. Bottom is simplified schematic of the microchannel network. (B) Example full-field image of binding experiment. A binding

reaction containing 100 nM c-di-GMP and 1 μM Alexa Fluor 488-labeled RNA was incubated for 60 min and was then loaded on a polyacrylamide gel run for 30 s at RT. (C) Analysis of equilibration time required for an excess of RNA to equilibrate with c-di-GMP. Binding reactions containing 100 nM c-di-GMP and 1 μM Alexa Fluor 488-labeled RNA were incubated for various times and were then loaded on a polyacrylamide gel run for 30 s at RT. (D) Standard curve of A33U Vc2 binding c-di-GMP. A binding reaction containing 1 μM Alexa Fluor 488-labeled RNA with various c-di-GMP concentrations was incubated for 60 min and was then loaded on a polyacrylamide gel run for 30 s at RT. In all studies, TI was used as an internal standard. A.F.U. stands for arbitrary fluorescence units.